

# Halogenated Materials as Organic Semiconductors<sup>†</sup>

Ming L. Tang<sup>‡,§</sup> and Zhenan Bao<sup>\*,‡</sup>

<sup>‡</sup>Department of Chemistry, University of California, Berkeley, California 94720, United States,  
<sup>§</sup>Materials Science Division, Lawrence Berkeley National Laboratory, 1 Cyclotron Road,  
Berkeley California 94720, United States, and <sup>‡</sup>Department of Chemical Engineering, Stanford University,  
Stanford California 94305, United States

Received August 2, 2010. Revised Manuscript Received October 18, 2010

Organic semiconductors have great potential as the active material in low-cost, large area plastic electronics, whether as light-emitting diodes (LEDs), field-effect transistors (FETs) or solar cells. Organic semiconducting materials retain the processability associated with polymers while maintaining good optoelectronic properties, for example, high absorption coefficients for photons in the visible, and field-effect mobilities comparable with that of amorphous silicon. The elucidation of important structure–property relationships is vital for the design of functional, high-performance organic semiconductors. In this short review, we summarize such relationships stemming from the halogenation of organic semiconductors. While it has been known in the past decade that fluorination lowers the energy levels in carbon based systems, induces stability and electron transport, less is known about the effect of the other halogens. Chlorination has recently been shown to be a viable route to *n*-type materials. The bandgap of conjugated compounds can also be decreased slightly by the addition of Cl, Br, and I to the aromatic core. The effect of the halogenated moieties on the packing of molecules is discussed.

## Introduction

Organic semiconducting materials are promising for large-area, low-cost electronic applications. These  $\pi$ -functional systems, the subject of this special issue, have optoelectronic properties that land themselves in applications such as light-emitting diodes,<sup>1,2</sup> transistors<sup>3–6</sup> and photovoltaic cells.<sup>7</sup> Compared to conventional semiconductors, organic semiconductors are amenable to solution-based, roll-to-roll processing techniques on flexible plastic substrates. Although inorganic nanocrystals have this feature in common as well, in comparison, organic materials are relatively easily scaled up and isolated in high purity. This is not only important for industrial purposes, but also allows elucidation of important structure–property relationships. This permits one to design molecules or polymers that are optimized for charge transport, light absorption, emission, etc.

In this short review, we discuss the effect of halogens on the electronic properties and solid state assembly of organic semiconducting materials. The stability of organic semiconductors, and the lack of *n*-type materials are two key issues hindering the commercialization of devices based on conjugated compounds. Recent reports indicate that halogenation may be a way around these problems.

Fluorination has been used in the past decade or two as a route to induce stability in organics by lowering both the highest occupied molecular orbital (HOMO) and the lowest unoccupied molecular orbital (LUMO) energy levels in the molecule or polymer, especially for organic

light-emitting diodes (OLEDs). The lowered energy levels facilitate electron injection, thus allowing the use of more stable cathodes like aluminum instead of the more reactive calcium.<sup>8</sup> Other advantages of fluorination are seen in organometallic iridium phenylpyridine complexes for OLEDs where the photoluminescence efficiency is enhanced by the reduction of nonradiative decay pathways. In addition, the sublimation temperature required to purify the compound decreases as well.<sup>9</sup> The reader is directed to a comprehensive review<sup>8</sup> of fluorinated poly(phenylenevinylene)s, poly(phenyleneethynylene)s, and polythiophenes mostly for OLED applications. These were polymerized from fluorinated monomers by Gilch type reactions, Wittig condensations and Stille or Suzuki–Miyaura cross-couplings.

In this review, we will discuss the impact of halogenation on (1) the packing of small molecules in thin film and the resulting thin film field-effect mobilities, (2) the energy levels of conjugated molecules and the empirical observation of the transition from *p*-type to ambipolar to solely *n*-type transport in field-effect transistors, and (3) the slight decrease in bandgap upon addition of chlorine, bromine, and iodine to the conjugated core. We begin first by reviewing the basic physical properties of carbon halogen bonds and theoretical considerations pertaining to charge transport, then move on to the synthesis of halogen containing oligomers. We then compare the effect of halogenation on different families of compounds, finally concluding with a section on halogenated compounds for solar cells.

<sup>†</sup> Accepted as part of the “Special Issue on  $\pi$ -Functional Materials”.

\*Corresponding author. E-mail: zbao@stanford.edu.

**Table 1. Atomic Electronegativities<sup>10</sup> of Hydrogen and the Halogens, Carbon–hydrogen and Carbon–halogen Homolytic Bond Dissociation Energies<sup>11</sup> in the Gas Phase, Bond Lengths, and Bond Dipole Moments<sup>12</sup>**

atomic electronegativities			bond dissociation energies (kcal mol <sup>-1</sup> )	bond length (Å)	bond moments (e.s. units × 10 <sup>18</sup> )
H	2.1	H <sub>3</sub> C–H	105	1.09	0.4
F	4.0	H <sub>3</sub> C–F	110	1.385	1.41
Cl	3.0	H <sub>3</sub> C–Cl	85	1.784	1.46
Br	2.8	H <sub>3</sub> C–Br	71	1.929	1.38
I	2.5	H <sub>3</sub> C–I	57	2.139	1.19

### Halogen Bond Energy and Polarity

The electronegative nature of the halogens results in molecules with polar bonds. In organic chemistry, the polarity of covalent bonds between carbon and its substituents forms the basis of structure–property relationships; this is true for organic semiconductors as well. In general, the larger the difference in electronegativity between atoms in a covalent bond, the larger the bond dipole. It is interesting to note that the dipole moment of the C–Cl bond is slightly larger than the C–F bond, even though F is much more electronegative than Cl. Carbon has a Pauling electronegativity of 2.5, the same as iodine. However, even though the carbon–iodine bond has no permanent dipole, it is very polarizable. This, in addition to the fact that the overlap of iodine p orbitals with carbon sp orbitals is the smallest among all the halogens in Table 1, explains why the carbon–iodine bond is the weakest carbon–halogen bond. It is not unusual to see the electrochemical reductive cleavage of carbon–iodine bonds. In fact, many iodinated conjugated molecules and some brominated ones are generally not stable. For example, in our hands, the sublimation of 2,3,9,10-tetrabromopentacene resulted in the loss of all bromines and the isolation of pentacene.

The extreme electronegativity of fluorine results in interesting parallel stacks in the solid state. We recall that quadrupole moments of benzene and hexafluorobenzene are large and opposite in sign. The quadrupole moment of benzene is large and negative,  $-29.0 \times 10^{-40}$  Cm<sup>2</sup> while that of hexafluorobenzene is large and positive at  $31.7 \times 10^{-40}$  Cm<sup>2</sup>.<sup>13</sup> The distribution of  $\pi$ -electron density above and below the benzene ring is inverted in hexafluorobenzene, due to the electronegativity of the F atoms. Molecular beam electric resonance spectroscopy reveals that a benzene/hexafluorobenzene dimer in the gas phase has an induced dipole moment of 0.44D,<sup>14</sup> implying a transfer of less than 1/8 electron between both molecules. In fact, although pure benzene crystallizes in the herringbone geometry to accommodate electric quadrupoles of like polarity, a 1:1 mixture of benzene/hexafluorobenzene stacks parallel to each other, each alternating with the other. In both cases, the molecules pack to maximize electrostatic attraction and minimize repulsion.<sup>15</sup>

This parallel stacking between benzene and fluorobenzene is observed in partially fluorinated conjugated molecules. Phenyl pentafluorophenyl interactions are observed in mixtures of *sym*-triphenylethynylbenzene and

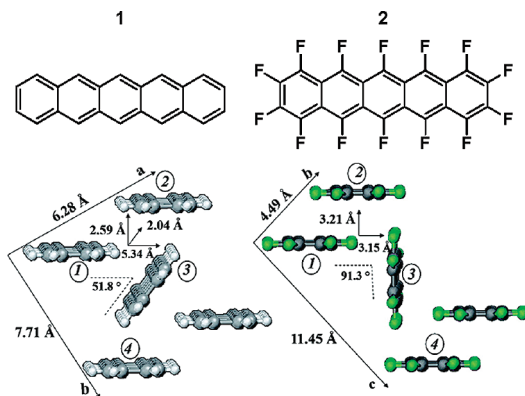


**Figure 1.** Illustration of the lattice parameters within the *ab* layer of single-crystal pentacene<sup>25</sup> and the *bc* layer of perfluoropentacene.<sup>19</sup> The short-axis and long-axis displacements along the  $\pi$ -stacks are also indicated. Figure adapted with permission from ref 22. Copyright 2009 American Chemical Society.

*sym*-tris(perfluorophenethynyl)benzene,<sup>16</sup> where the individual molecules pack in slip stacks with slip angles of 46–48°. A 1:1 mixture of the above two compounds instead forms columnar stacks, each alternating with the other and a slip angle of 20°. Watson and co-workers reported another example, where their partially fluorinated tetracyclic discs pack in parallel with each other, with a slight lateral offset between adjacent molecules, in line with calculated molecular electrostatic potentials.<sup>17</sup> They have also made a series of differently fluorinated benzobisbenzothiophene, which show close thienyl sulfur–fluorine contacts.<sup>18</sup> They attribute the small interplanar distance between molecules to S–F interactions.

### Theoretical Considerations

The synthesis of perfluoropentacene<sup>19</sup> and tetradecafluorosexithiophene<sup>20</sup> by Suzuki and co-workers have prompted theorists to explain the experimentally determined field-effect mobilities. Calculations have also been performed for 1,4-diiodobenzene after Ellman and co-workers measured a high time-of-flight hole mobility of 12 cm<sup>2</sup>/(V s) in single crystals.<sup>21</sup> Unfortunately, not much has been calculated for chlorine or bromine-functionalized molecules, probably because they have only recently been reported. This section summarizes the results of these studies.

Many groups have found that perfluorination stabilizes frontier molecular orbitals, increases the stability of the radical anion, and decreases the barrier for electron injection. In addition to these molecular properties, the reorganization energies and transfer integrals can be calculated for a thin film if the structural parameters are known. It was found that the reorganization energy from the geometrical relaxation when charges traverse from molecule to molecule doubles going from pentacene (1 in Figure 1) to perfluoropentacene (2 in Figure 1).<sup>22,23</sup> This is attributed to the increased vibronic interactions of holes and electrons with C–C/C–F stretching modes. However, both the hole and electron reorganization energy is virtually unchanged going from sexithiophene (6T) to tetradecafluorosexithiophene,<sup>23</sup> (13, Figure 3). The authors attribute this to the fact that while 6T is twisted in its neutral

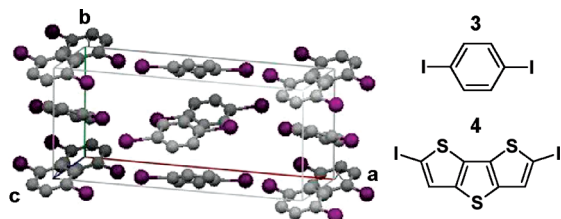


**Figure 2.** Crystal structure of the  $\alpha$  phase of 1,4-diiodobenzene, **3**<sup>30</sup> ( $Pbca$  space group,  $a = 16.9697$ ,  $b = 7.3242$ , and  $c = 6.156$  Å). The chemical structure of 1,4-diiodobenzene, **3** (upper right), and 2,6-diiododithieno[3,2-*b*:2',3'-*d*]thiophene, **4** (lower right).

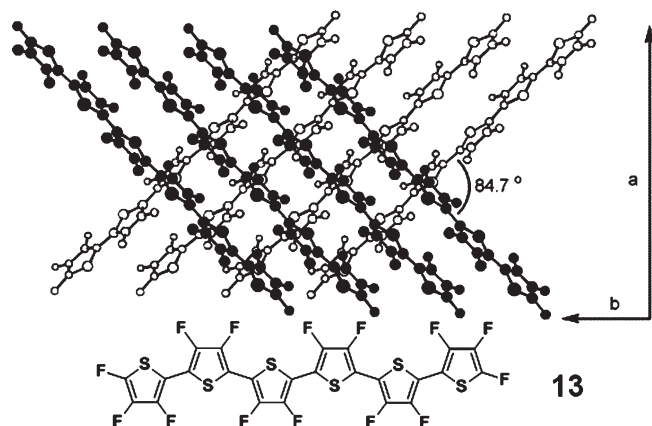


**Figure 3.** Single-crystal structure of tetradecafluorosexithiophene.<sup>20</sup> Figure adapted with permission from ref 20. Copyright 2001 American Chemical Society.

state with a dihedral angle of 16.5° between adjacent thiophene rings, the quinodal forms of hole and electron transporting 6T are planar. In comparison, the excited and neutral states of linear acenes are planar. Similarly, the intramolecular reorganization energy for partially fluorinated tetracene derivatives is larger than that of tetracene, though less than that of alkoxy-substituted molecules.<sup>24</sup>

The single-crystal structures of pentacene and perfluoropentacene are shown in Figure 1. Pentacene displays the familiar herringbone packing, with an angle of 52° between molecular planes along the herringbone diagonal axis, while perfluoropentacene molecules are nearly perpendicular  $\sim 91^\circ$  along the same direction. The interplanar distance between the  $\pi$ -stacks in pentacene along the  $a$  direction (2.55 Å) is smaller than the 3.25 Å in the  $b$  direction in perfluoropentacene. However, this is mitigated by the fact that there is more overlap along the short axis of the molecules (molecule 1 and 2 in Figure 1) along this direction for perfluoropentacene, resulting in a hole[electron] transfer integral four [two] times larger than pentacene along the same direction.<sup>22</sup> Having noted that, to date, perfluoropentacene has displayed electron transport only in FET devices, with an electron mobility of 0.22 cm<sup>2</sup>/(V s),<sup>19</sup> whereas pentacene routinely gives hole FET mobilities on the order of 0.5–1 cm<sup>2</sup>/(V s). Indeed, it would be more pertinent to compare structural parameters of both molecules in the thin film phase,<sup>26</sup> rather than the single-crystal phase.

Calculations comparing fluorinated and chlorinated dithieno[2,3-*b*:2',3'-*d*]thiophenes<sup>27</sup> show that the reorganization

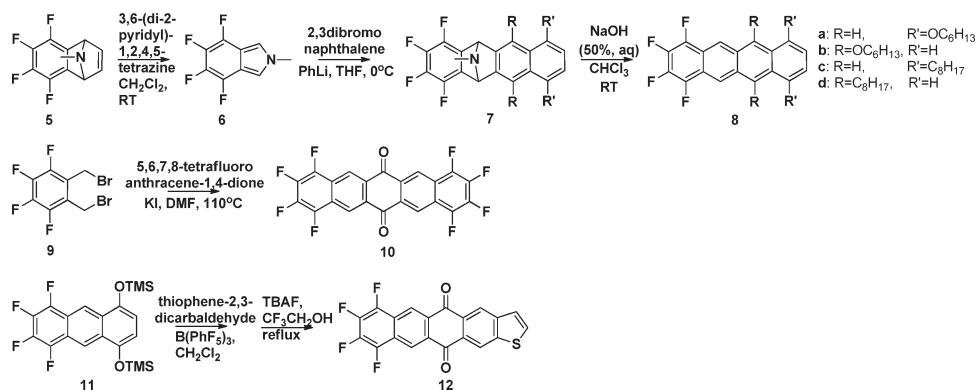
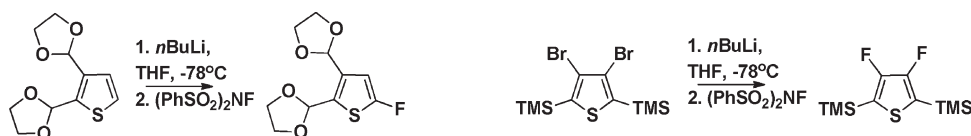
energy for holes does not differ much from the parent molecule, but that the electron reorganization energy almost triples for fluorinated molecules and increases by an order of magnitude when derivatized with chlorine. The asymmetry in hole and electron reorganization energies upon halogenation was not addressed.

Although reorganization energies were found to increase with fluorination and chlorination, the opposite is true for hole reorganization energies calculated for two iodinated molecules, 1,4-diiodobenzene, **3**, and 2,6-diiododithieno[3,2-*b*:2',3'-*d*]thiophene, **4**, (Figure 2). For example, the intramolecular reorganization energy for 2,6-diiododithieno[3,2-*b*:2',3'-*d*]thiophene is 20% smaller than the parent molecule,<sup>28</sup> though approximately 3 times larger compared to that calculated for pentacene. Similarly, compared to benzene, a very small effective mass of 0.5 $m_0$  was calculated for both charge carriers in 1,4-diiodobenzene along the  $a$ -axis.<sup>29</sup> In comparison, the same group found a value of 0.8 $m_0$  for rubrene. These seemingly contradictory findings (at least compared with the fluorinated molecules) stem from the fact that iodine is very heavy and does not readily contribute to intramolecular vibrations that result in local electron–phonon couplings. Therefore the hole-vibration coupling constants of stretching modes involving iodine atoms are diminished.

The high hole mobility in 1,4-diiodobenzene is also explained by the reduction in hole polaron binding energy<sup>29</sup> (40% less than benzene). The calculations reproduced the experimentally measured anisotropy of the hole mobility in this molecule, where the lightest effective mass was found along the  $a$ -axis which has the shortest intermolecular distance between the iodine atoms. This is in direct opposition to the finding that in 2,6-diiododithieno[3,2-*b*:2',3'-*d*]thiophene, **4**, the effective mass is largest along the  $c$ -axis where the intermolecular distance between iodine atoms are the shortest.<sup>28</sup> Electron mobilities are not expected to be observed in either compounds because of the facile cleavage of the carbon–iodine bond in the anionic radical form of the molecules, as seen in the electrochemical decomposition of 2,6-diiododithieno[3,2-*b*:2',3'-*d*]thiophene.<sup>28</sup>

There is a significant bathochromic shift upon functionalizing conjugated molecules with iodine. For example, the HOMO–LUMO gap in 1,4-diiodobenzene is 1.4 eV smaller than benzene,<sup>29</sup> whereas there is a red shift of 0.35 eV going from dithienothiophene to the 2,6-diiodinated compound.<sup>28</sup> This red shift is attributed to the inductive effect of iodine which lowers the LUMO level with respect to the parent molecule, as well as iodine atoms behaving as  $\pi$ -electron donors. This is consistent with the observation of a similar bathochromic shift when acenes are partially chlorinated.<sup>31</sup> Density functional theory (DFT) calculations reveal that the LUMO has contributions from the halogens.  $\pi$ -electrons partially delocalize onto the halogen, perhaps on to the empty d-orbitals, resulting in a red shift. Such observations are not seen in fluorine functionalized molecules because it does not have energetically accessible d-orbitals for this delocalization of  $\pi$ -electrons.



Scheme 1. Synthesis of Linear Acenes with Csp<sup>2</sup>–F Bonds<sup>34–36</sup>Scheme 2. Electrophilic Aromatic Fluorination of Thiophenes That Are Precursors to  $\alpha$ -Fluorinated Anthradithiophene<sup>39</sup> (left) and Tetradecafluorothiophene<sup>20</sup> (right)

### Preparation of Halogenated $\pi$ -Compounds

The selective formation of carbon–fluorine bonds, especially Csp<sup>2</sup>–F bonds, remains a challenge, and these excellent reviews cover the latest developments in transition metal mediated coupling.<sup>32,33</sup> The difficulty lies in the reductive elimination step when electron deficient species are used. Therefore most compounds with fluorine atoms are made from heavily halogenated precursors. As mentioned before, the synthesis of partially fluorinated conjugated polymers, made by polymerizing fluorinated monomers, for organic LED applications is summarized elsewhere.<sup>8</sup> This section will be an overview of syntheses of halogenated planar molecules that have potential for transistor applications.

Tetrafluorinated benzene precursors have been used to make linear acenes, as demonstrated by the Swager,<sup>34</sup> Anthony,<sup>35</sup> and Bao<sup>36</sup> groups. Scheme 1 shows work by Chen et al.,<sup>34</sup> who used a Diels–Alder reaction followed by a thermally allowed electrocyclic fragmentation to make **6** from **5**. Then a second Diels–Alder reaction occurred with naphthalene, giving **7**, which could be deaminated by an in situ generated dichlorocarbene that gave an ammonium ylide. Aromatization proceeded by the facile cheletropic loss of methyl isocyanide dichloride to give **8**. Swartz and co-workers used the Cava reaction to generate the quinodimethanes in situ to react with internal quinones,<sup>35</sup> as shown in Scheme 1, from **9** to **10**. Their group and our group independently found that the 4-fold aldol condensation between a phthalaldehyde and 1,4-cyclohexanedione (that is commonly used to make pentacene and its tetrachloro<sup>37</sup> and tetramethyl derivatives) resulted in negligible yield with fluorinated precursors. 2,3,9,10-tetrachloropentacene was made by condensing 4,5-dichlorophthalaldehyde with 1,4-cyclohexanedione.<sup>37</sup> We used the Mukaiyama aldol condensation with an aromatic silyl enol ether, **11**,

in the presence of a Lewis acid catalyst to make **12**, the asymmetric 7,8,9,10-tetrafluoro-tetraceno[2,3-*b*]thiophene-5,12-dione,<sup>36</sup> (Scheme 1) as well as its tetrachlorinated isomer.

Electrophilic fluorine substitution can be achieved with reagents like Selectfluor,<sup>38</sup> a stable, crystalline, nonhydroscopic solid. A similar reagent, *N*-fluorobenzene sulphonamide has been used to fluorinate thiophenes, as shown in Scheme 2.<sup>20,39</sup> The resulting molecules show a slight blue shift in their optical spectra compared to the parent molecules.

The Suzuki group's synthesis schemes of perfluoropentacene and tetradecafluorosexithiophene are illustrated in Scheme 3. With so many electron-withdrawing fluorine atoms, the LUMO of perfluoropentacene was found by differential pulse voltammogram (DPV) to be almost the same as that of C<sub>60</sub>, which explains why hole transport has not been observed with this molecule. The HOMO–LUMO gap of perfluoropentacene was found to be red-shifted by 0.12 eV, whereas the emission maxima in -dichlorobenzene was 652 nm, red-shifted by 63 nm compared to pentacene.

Stille coupling can be used with stannylated aryls containing perfluoroalkyl groups<sup>40</sup> or perfluoroarenes,<sup>41</sup> whereas Ullman coupling can be used with bromoperfluoroarenes (see Scheme 3).<sup>42</sup> Facchetti and Marks have made a variety of fluoroarene<sup>43</sup> and perfluoroalkyl containing thiophenes. The synthesis of their fluorinated precursors is shown in Scheme 4. Using copper-catalyzed coupling between perfluoroiodides and arylbromides,<sup>40</sup> they made building blocks for a series of *n*-type thiophenes with up to six aromatic units. The copper-mediated reaction was used to make bis-(perfluorobutyl)pentacene<sup>44</sup> and perfluorinated oligophenyls with up to seven phenyl units.<sup>42</sup> A transition-metal-free, fluoride-activated coupling between trimethylsilyl-functionalized thiophene and perfluorobenzene or perfluoronaphthalene

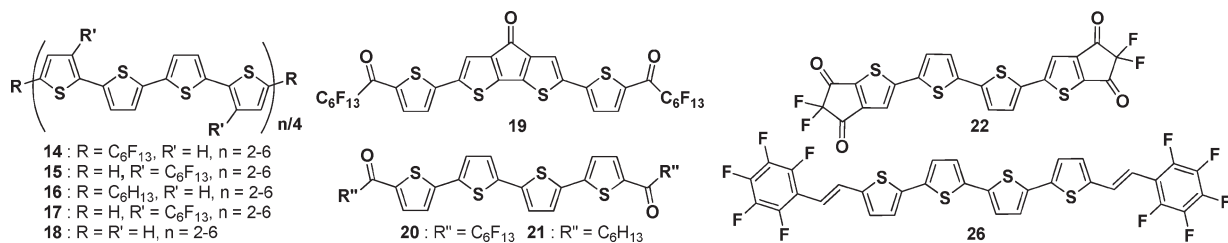
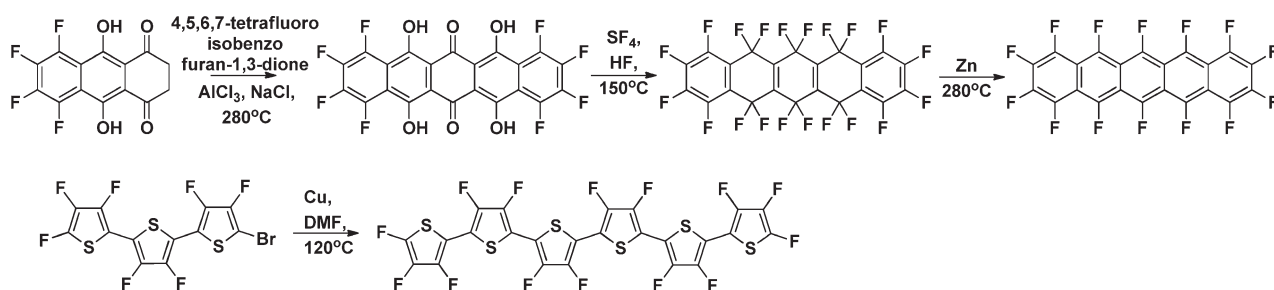
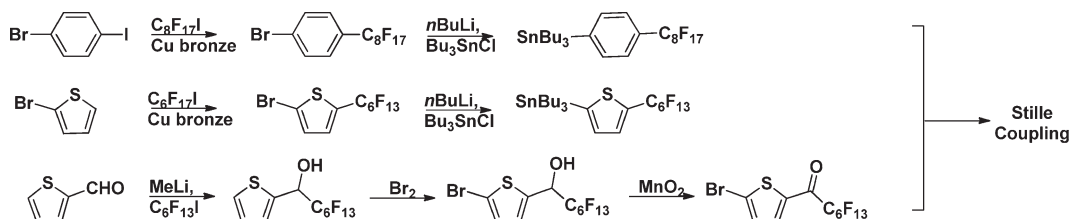


**Figure 4.** Family of perfluorohexyl/hexyl thiophenes (14–18)<sup>40,51</sup> and their carbonyl containing relatives (19–21),<sup>52</sup> *n*-type difluorodioxocyclopentene-annulated quarterthiophene,<sup>53</sup> 22, and *p*-type perfluoroarenestrylquarterthiophene,<sup>54</sup> 26.

**Scheme 3. Synthesis of Perfluoropentacene<sup>19</sup> (top), and Ullman Coupling Leading to Tetradecafluorothiophene<sup>20</sup> (bottom)**



**Scheme 4. Perfluoroalkyl Functionalization of Aryl Iodides and Bromides Mediated by Copper, Which Lead to *n*-Type Quarter, Penta, and Hexathiophenes via Stille Coupling<sup>40–43</sup>**



seems to be a facile route to perfluoroarene-containing oligomers.<sup>45</sup>

Perylene 3,4,9,10-tetracarboxylic bisimide (PTCDI) dyes are good *n*-type semiconductors as they have relatively low LUMO levels. However, to induce operation in air, either the imide substituents must be fluorinated or the aromatic portion must be fluorinated, chlorinated, or cyanated. The Halex reaction was utilized for fluorinating the perylene bay positions by using potassium chloride in sulfolane and various catalysts,<sup>46</sup> whereas complete chlorination of the perylene core was achieved with chlorosulfonic acid at 80 °C, to give Cl<sub>8</sub>-PTCDI.<sup>47</sup> Bromo-core-substituted arylene diimides can be functionalized via Stille coupling<sup>48</sup> or copper-mediated perfluoroalkylation.<sup>49</sup>

In light of the fact that chlorination is a viable route to *n*-type materials,<sup>31,47</sup> and chlorine synthesis being more developed than fluorine, perhaps we will see more examples of such molecules in the future.

**Thin Films of Halogenated  $\pi$ -Compounds**

This section compares the halogenated molecules to their parent compounds in terms of their single-crystal and thin-film packing parameters and their resulting FET properties.

**Thiophenes.** Sexithiophene and tetradecafluorosexithiophene (13, Figure 3) have drastically different single-crystal

structures. Although sexithiophene packs in the familiar herringbone geometry,<sup>50</sup> its fluorinated counterparts has a face-to-face  $\pi$ -stacked structure with a tilt angle of 84.7° between adjacent stacks, as shown in Figure 3. The authors speculate that this is due to the dipole–dipole interactions in the fluorinated molecule.

The oligothiophenes with alkyl and perfluoroalkyl side chains, whether on the  $\alpha,\omega$  (14, 16 in Figure 4) or the  $\beta,\beta'$  (15, 17 in Figure 4) positions essentially display a similar kind of solid state organization to dihexylsexithiophene,<sup>50</sup> with segregation of conjugated core and aliphatic substituents.<sup>51</sup> The fluorocarbon and alkyl functionalized oligothiophenes have virtually indistinguishable microstructures, with similar *d* spacings and molecular tilt orientations. Compared to  $\alpha$ -sexithiophene, *n*-hexyl groups raise molecular energy levels by 0.11 eV, whereas *n*-perfluorohexyl groups lower both the HOMO and LUMO by around 0.40 eV. There is, however, a hypsochromic shift from the alkyl (16 in Figure 4) to the perfluoroalkyl (14 in Figure 4) in the UV–vis absorption (5–31 nm) and emission (0.2–0.4 eV) spectrum.<sup>40</sup> In addition, thin films of perfluoroalkyl substituted oligothiophenes have significantly greater emission quantum efficiencies. The authors attribute this to the fact that perfluoroalkyl side chains facilitate emission from a higher energy excited state by preventing fast nonradiative decay into the lowest

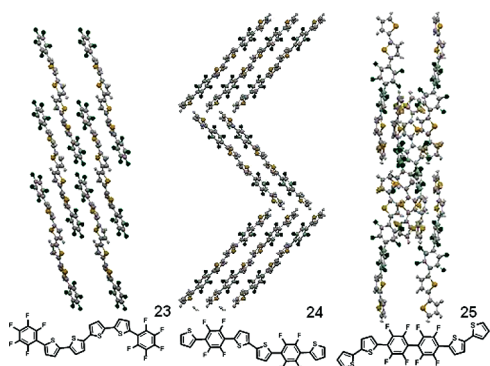


**Figure 5.** Single-crystal structures of isomers of bisfluoroarene-quarterthiophene oligomers. Molecule **23** is *n*-type, whereas **24** and **25** are *p*-type, as measured in Argon. **25** has very poor charge transport properties.<sup>43</sup> Figure adapted with permission from ref 43. Copyright 2003 Wiley.

excited state, as their absorption and emission profiles are similar to their alkyl cousins but blue-shifted. In terms of FET devices, the perfluoroalkyl functionalized oligothiophenes were *n*-type materials, whereas the alkyl versions were *p*-type. In general, devices from perfluoroalkyl oligothiophenes, compared to alkylated oligomers with the same degree of conjugation, had lower mobilities, but were more stable with lower off currents.<sup>51</sup> The best performing *n*-type FETs were from diperfluorohexylquarterthiophene (**14** in Figure 4, where  $n = 16$ ) with an electron mobility of  $0.22 \text{ cm}^2/(\text{V s})$  in vacuum.

As expected from the considerable twisting between thiophene rings in the  $\beta$ ,  $\beta'$  (**15**, **17** in Figure 4) series, the UV–vis absorption maxima is blue-shifted from the oligothiophenes with end substitutions. Interestingly, in thin films, this series shows a red-shift compared to the end substituted counterparts. It is postulated that this series of  $\beta$ ,  $\beta'$ -substituted molecules form H-type aggregates because they have more significant coupling between molecular transition dipoles.<sup>40</sup>

Carbonyl groups were used to further lower molecular energy levels to give air stable *n*-type quarterthiophenes, as drawn in Figure 4. Molecules **19** and **20** display only *n*-type transport on hexamethyldisilazane (HMDS) treated substrates with electron mobilities of up to  $0.6 \text{ cm}^2/(\text{V s})$  (vacuum) and  $0.02 \text{ cm}^2/(\text{V s})$  (air), while molecule **21** shows ambipolar transport with hole and electron mobilities of  $0.01$  and  $0.1 \text{ cm}^2/(\text{V s})$ , respectively. **22**, the difluorodioxocyclopentene-annelated quarterthiophene gave an electron mobility of  $0.013 \text{ cm}^2/(\text{V s})$ .<sup>53</sup>

Figure 5 shows three isomers consisting of four thiophene and two fluoroarene units made by Facchetti and co-workers. The crystal structures of these oligomers show close cofacial stacks where the electron rich thiophene units overlap with the electron poor fluoroarene entities,<sup>43</sup> in contrast to the herringbone packing motif of perfluoroalkyl/alkyl thiophenes and phenylene-thiophene oligomers. Compared to the phenylene-thiophene oligomers, the fluoroarene containing molecules show a 5–11 nm hypsochromic shift.<sup>55</sup> Molecules **23** and **24** have a minimum cofacial  $\pi$ – $\pi$  distance of 3.20 and 3.37, Å respectively, comparable to Anthony's  $\pi$ -stacked 6,13-triisopropylsilylacetylenepentacene molecule. Interestingly,

**23** displays pairs of thiophenes *syn* to each other, which is quite uncommon. **23** has an electron mobility of  $0.5 \text{ cm}^2/(\text{V s})$ ,<sup>55</sup> whereas **24** and **25** have holes mobilities of  $0.005$  and  $0.00002 \text{ cm}^2/(\text{V s})$ , respectively, with no ambipolar behavior observed.<sup>55</sup> Calculations reveal that the electron injection into the oligomer with perfluoroarenes on the ends of the molecule is favored, but ambipolar charge transport is expected for the other perfluorophenylthiophene oligomers as well.<sup>56</sup> Surprisingly, **26** (Figure 4), a quarterthiophene very similar to **23** transports only holes.<sup>54</sup> The authors fault the double bond for confining most of the spin density at the fluorobenzene ends of the molecule, thus thwarting the  $\pi$ -conjugation. However, they do concede the poor morphology of their evaporated thin film might be the cause as well.

A series of *n*-perfluorooctyl-capped phenylene-thiophene oligomers with up to six aromatic units make thin films that show *n*-type behavior and high current  $I_{\text{on}}$ :  $I_{\text{off}}$  ratios. In this series, the best electron mobility of  $0.1 \text{ cm}^2/(\text{V s})$  was observed for 5,5'-bis(4-*n*-perfluorooctylphenyl)-2,2'-bithiophene. At that time, this molecule displayed the largest transistor memory effect reported for organics. Trifluoroacetyl groups at the periphery of this conjugated core gives electron transporting FETs as well.<sup>57</sup>

A related series of thiophene and selenophene copolymers with phenylene, difluorophenylene or tetrafluorophenylene units in the main chain were compared against each other,<sup>58</sup> and it was found that the tetrafluorinated version performed best, in terms of hole mobility, ambient stability, and film formation properties. The monomers were found to pack in slip stacks, with the tetrafluorophenylene unit in close proximity to the thiophene ring of a neighboring molecule.

The trifluoromethylphenyl group has been used with great utility in making high mobility *n*-channel transistors. The 5,5'-bithiazole with trifluoromethylphenyl end groups forms two-dimensional columnar stacks with mobility of  $1.83 \text{ cm}^2/(\text{V s})$ ,<sup>59</sup> whereas the 5,5'-bithiophene version has a mobility of  $0.18 \text{ cm}^2/(\text{V s})$  with a herringbone structure.<sup>60</sup>

**Acenes.** Hexafluoro-hexa-*peri*-hexabenzocoronene has molecular energy levels  $0.4 \text{ eV}$  lower than its parent molecule, with the HOMO–LUMO gap unchanged.<sup>61</sup> The interface dipole with Cu(111) was estimated to increase from  $+0.2$  to  $+0.9 \text{ eV}$  upon fluorination. Such positive interface dipoles are commonly observed between  $\text{C}_{60}$  and  $\text{CuPcF}_{16}$  and metals.

A fluorine atom on the  $\alpha$  position of the thiophenes for the triethylsilylthynyl-anthradithiophene resulted in a more stable molecule with a slightly higher bandgap. This molecule gave hole mobilities  $> 1 \text{ cm}^2/(\text{V s})$  when deposited on perfluorobenzenethiol-treated gold electrodes for devices with very small channel lengths.<sup>39</sup>

Single crystals of mono, di, and tetrachlorotetracene have been fabricated. 5,6,11,12-Tetrachlorotetracene<sup>62</sup> and 5,11-dichlorotetracene<sup>63</sup> both display the face-to-face slipped  $\pi$  stacking with similar pitch and roll angles and interplanar distances of 3.56 and 3.485 Å, respectively.



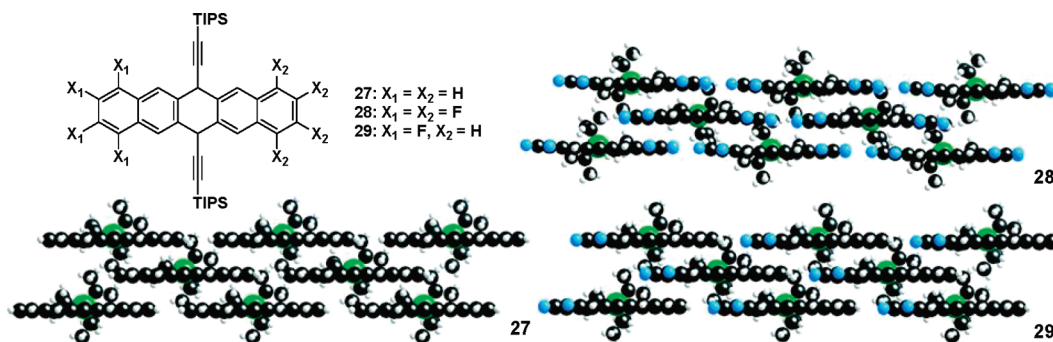


**Figure 6.** Two-dimensional  $\pi$ -stacked structure of 6,13-TIPSEthynylpentacene, **27**, with the octafluoro, **28**, and tetrafluoro, **29**, derivatives.<sup>35</sup> Figure adapted with permission from ref 35. Copyright 2005 American Chemical Society.

The dichlorinated molecule had a single-crystal mobility of  $1.6 \text{ cm}^2/(\text{V s})$ , whereas the tetrachlorinated one has mobilities of  $0.2 \text{ cm}^2/(\text{V s})$ . The 5-chloro and 5-bromo tetracene derivatives pack in the herringbone geometry and did not show equivalent charge-transport characteristics.

Pentacene has been partially brominated and chlorinated at the 2,3 positions. 2-Bromo, 2,3-dibromo, and 2- $\text{CF}_3$ -pentacene show a red shift in their UV-vis absorption spectrum compared to pentacene.<sup>64</sup> Of these, the 2,3-dibromopentacene had the highest mobility of  $0.23 \text{ cm}^2/(\text{V s})$  and was stable in air for a period of 80 days while a pentacene FET made under the same conditions rapidly deteriorated. 2,9-diperfluorobutylpentacene is an *n*-type material with an electron mobility of  $0.0017 \text{ cm}^2/(\text{V s})$  with Ag electrodes.<sup>44</sup> Wudl et al. observed the loss of 2 chlorine atoms from each 2,3,9,10-tetrachloropentacene to give a poly(iptycene) ladderlike polymer at  $400^\circ\text{C}$  from a clean Diels-Alder coupling.<sup>37</sup>

Fluorinated 6,13-TIPSEthynyl-pentacene derivatives were first synthesized by Anthony and co-workers.<sup>35</sup> As seen in Figure 6, the bulkiness of the TIPS group enforces a two-dimensional,  $\pi$ -stacked structure. The addition of fluorine atoms on the peripheral ring(s) of pentacene decreases the average interplanar spacing from  $3.43 \text{ \AA}$  for the unfluorinated **27** to  $3.36 \text{ \AA}$  for the tetrafluoro **29** and  $3.28 \text{ \AA}$  for the octafluoro compound **28**. There is a red shift of  $\sim 7 \text{ nm}$  from **27** to the partially fluorinated **28** and **29**.

The transition of charge-carrier type in organic FETs, from hole only, to ambipolar, to electron only transport were mapped out in acenes with the synthesis of halogenated compounds.<sup>65</sup> Fluorination, chlorination and bromination<sup>66</sup> of the tetraceno[2,3-*b*]thiophene core allowed systematic tuning of energy levels in a series of 16 molecules.<sup>67</sup> These, combined with Anthony's and Suzuki's fluorine containing pentacene molecules, resulted in 19 functionalized linear acenes that had LUMO levels between  $-2.8$  to  $-3.7 \text{ eV}$ , and HOMO levels from  $-4.9$  to  $-5.6 \text{ eV}$ . Top-contact FETs made with gold electrodes on octadecyltrimethoxysilane (OTS) treated thermally grown silicon substrates allowed comparison of the electronic properties of the active layer. Electron injection and transport occur when the LUMO  $< -3.15 \text{ eV}$ , while hole injection and transport occur when the HOMO  $> -5.6 \text{ eV}$ . Ambipolar transport is observed for molecules with

HOMO and LUMO levels within that range, as shown in Figure 7. In fact, the halogenated TIPSEthynylpentacene and tetraceno[2,3-*b*]thiophene molecules have high and balanced hole and electron mobilities. It is postulated that this empirical trend exists for a given dielectric, electrode, and family of molecules.

Chlorination of conjugated compounds is a practical route toward *n*-type materials.<sup>31</sup> This can be seen by comparing various aromatic cores that are functionalized in the same positions with either fluorine or chlorine atoms. In the acene family, the tetrachloro/fluoro TIPSEthynylpentacene and TIPSEthynyltetraceno[2,3-*b*]thiophene molecules (molecule **XVII** and **XVI**; **XIII** and **XV** respectively in Figure 7) both show ambipolar transistor behavior, with the chloro-containing molecules displaying equivalent or better mobility. For the copper phthalocyanines, the hexadecylchloro derivative, **Cl<sub>16</sub>CuPc** has an electron mobility of  $0.11 \text{ cm}^2/(\text{V s})$  in air on OTS treated substrates<sup>68</sup> compared to  $0.03 \text{ cm}^2/(\text{V s})$  for **F<sub>16</sub>CuPc** on untreated  $\text{SiO}_2$ .<sup>69</sup> If the chlorine atoms added do not distort the planarity of the conjugated core, then a red shift is observed from the parent molecule. This is consistent with the inductive effect of chlorine, and  $\pi$ -electrons delocalizing onto empty d-orbitals on the halogens. DFT calculations show that the HOMO and LUMO have contributions from the chlorine atoms.<sup>31</sup>

**Arylene Diimides.** A high electron mobility of  $0.82 \text{ cm}^2/(\text{V s})$  was recently reported for PTCDI octachlorinated (**Cl<sub>8</sub>PTCDI**) in all its aromatic positions<sup>47</sup> (**30** in Figure 8). This high mobility was attributed to the hydrogen bonding that resulted in a slipped two-dimensional  $\pi$ -stacked layer with the shortest interplanar distance of  $3.4 \text{ \AA}$ . In the third dimension, close chlorine-chlorine atoms between neighboring molecules are thought to enhance electron transport. A structural analogue where the amide groups were replaced with anhydride groups (thus precluding hydrogen bonding) showed mobilities 4 orders of magnitude lower. With these eight chlorine atoms, the LUMO is estimated at  $-4.23 \text{ eV}$ , compared to  $-3.8 \text{ eV}$  for the 1,6,7,12-tetrachloro-substituted PTCDI (**Cl<sub>4</sub>PTCDI**, **31** in Figure 8), and  $-3.7 \text{ eV}$  for the parent compound. **Cl<sub>4</sub>PTCDI** has a lower mobility of  $0.1 \text{ cm}^2/(\text{V s})$  in air,<sup>70</sup> though it packs in a similar way. Both molecules, as well as the tetrafluoro analogue, **F<sub>4</sub>PTCDI**<sup>71</sup> (**32** in Figure 8), show secondary phases in XRD of the thin films. Other than the primary phase, polymorphs due to

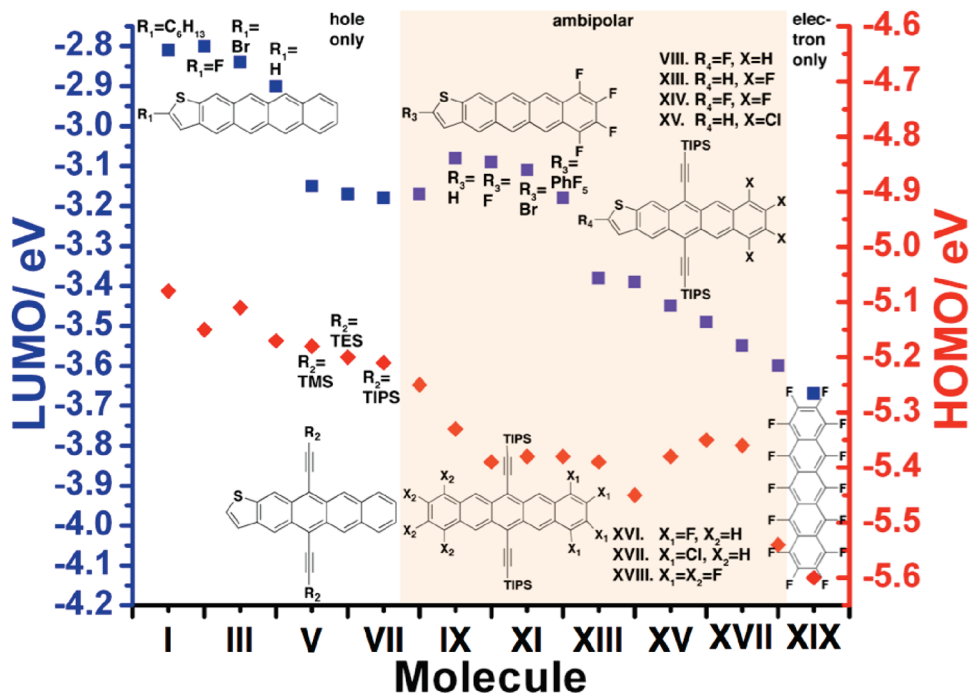


**Figure 7.** Functionalized pentacene and tetraceno[2,3-*b*]thiophene molecules with a range of HOMO (right y-axis, red diamonds) and LUMO (left y-axis, blue squares) levels. The top-contact FETs vary from those that display hole-only transport, to ambipolar, to electron-only transport depending on frontier molecular energy levels.<sup>65</sup> Figure adapted with permission from ref 65. Copyright 2009 American Chemical Society.

the P and M atropo-enantiomers may arise from the distorted, nonplanar perylene cores of these molecules.

Schmidt et al made a series of PTCDis, and molecule **33** (Figure 8) turned out to have the best FET characteristics, with electron mobilities  $> 1 \text{ cm}^2/(\text{V s})$  in air and high current  $I_{\text{on}}/I_{\text{off}}$  ratios.<sup>46</sup> **36** and **37** with chlorination and bromination at two of the bay positions respectively showed lower FET mobilities than **35**, the fluorinated version, which was relatively planar. Interestingly, **37** showed the largest reduction potential among molecules in this series, even though Br is the least electro-negative of the halogens used.

Naphthalene tetracarboxylic diimides (NTCDI) that are air stable have either (1) perfluorooctyl groups or trifluoromethyl groups at the imide positions;<sup>72</sup> or (2) cyano groups at the bay positions. The former are shown in Figure 8 (**38** and **40**), and have electron mobilities of  $0.01 \text{ cm}^2/(\text{V s})$  in air, whereas their unhalogenated analogues (**39** and **41** respectively) are not air stable. *N,N'*-bis(*n*-octyl)-2,6-dicyanonaphthalene-1,4,5,8-bis(dicarboximide) has a very low LUMO level of  $-4.5 \text{ eV}$  that explains its high electron mobility of  $0.15 \text{ cm}^2/(\text{V s})$  in air.<sup>73</sup>

The role of fluorinated side chains or substituents in making air-stable *n*-type FETs is still under debate. In 2000, Katz reported that due to a larger van der Waals radii than their hydrocarbon counterparts, perfluoroalkyl side chains result in a barrier to oxygen and water that stabilize electron transport in NTCDI derivatives.<sup>74</sup> However, the rate of mobility degradation in air was the same for thin films of 5 core-cyanated PTCDis irrespective of the original morphology,<sup>75</sup> thus lending less credence to that theory. Empirically Jones and co-workers

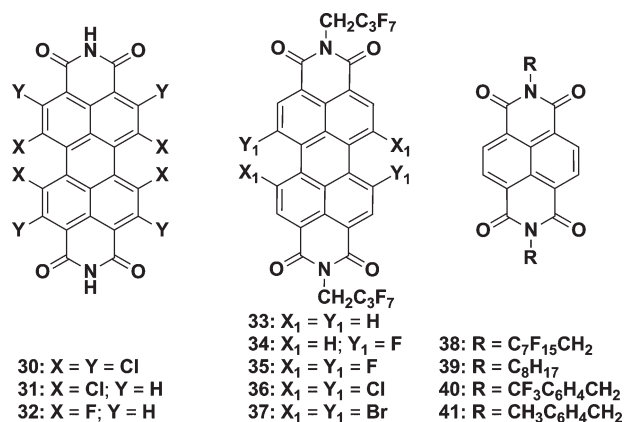


**Figure 8.** Halogenated PTCDis (left and middle) and NTCDIs (right) discussed.<sup>46,47,70,71</sup>

report that a reduction potential in excess of  $-0.1 \text{ V}$  vs SCE results in air-stable electron transport for their PTCDI and NTCDI derivatives.<sup>73</sup> We have found that thin films less than four monolayers thick of (*N,N'*-bis(cyclohexyl)-1,7-dicyano-perylene-3,4,9,10-tetracarboxylic acid diimide, whose LUMO =  $-0.07 \text{ V} > -0.1 \text{ V}$  vs SCE did not yield air-stable transistors, but thicker films worked well in air.<sup>76</sup> A convolution of both morphological and energetic factors must affect the stability of fluorinated devices in air.

**Halogenated Compounds in Organic Solar Cells.**  $\text{C}_{60}$  and [6,6]-phenyl C61-butyric acid methyl ester (PCBM) remain the quintessential electron transporting material used in organic solar cells. Efforts to find alternatives that are air-stable and have better charge-transport properties are underway. Figure 9 shows some fluorine containing PCBM derivatives that have been characterized in FETs.<sup>77,78</sup>



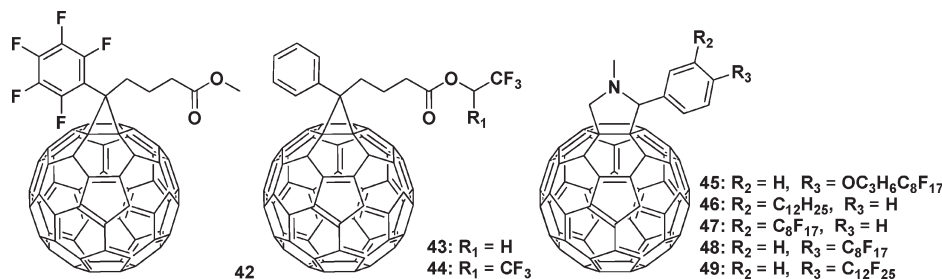


**Figure 9.** Fluorinated PCBMs.<sup>78</sup> PCBM **49** FETs can operate in air, whereas other  $C_{60}$  derivatives can not.<sup>77</sup>

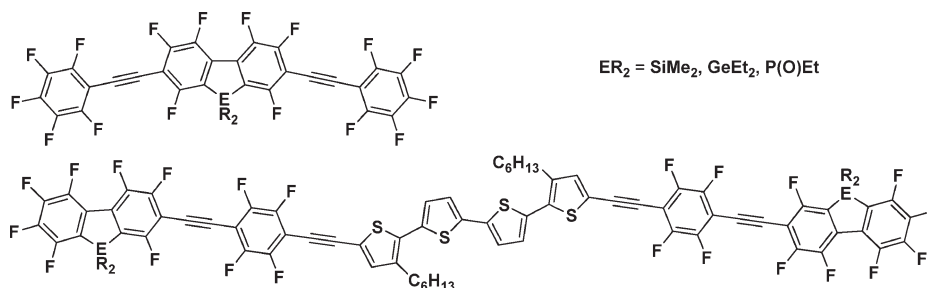


**Figure 10.** Donor–acceptor hexafluoroheterofluorenes oligomers for solar cell applications.<sup>79,80</sup>

PCBMs **42–45** do not form crystalline films, whereas PCBMs **46–49** do because of their long alkyl chains. Fluorination does enhance the stability of thin films formed, as PCBM **49** can operate in air as an  $n$ -type transistor with mobilities only three times smaller than that measured under vacuum ( $0.22 \text{ cm}^2/(\text{V s})$ ). This enhanced stability is attributed to the presence of long perfluoroalkyl chains that limit the diffusion of electron traps like oxygen, as the LUMO level of PCBM **49** is the same as PCBM.<sup>77</sup>

Figure 10 below shows examples of perfluoroarene containing oligomers with heterofluorenes.<sup>79,80</sup> These compounds were made by nucleophilic aromatic substitution and palladium-catalyzed coupling reactions. The hexafluoroheterofluorenes molecules do not form uniform films when solution processed. Single-crystal structures show that all of them have cofacial  $\pi$  stacks with distances of 3.2–3.7 Å between heterofluorene moieties of adjacent molecules. Using these compounds instead of PCBM in thin films for organic solar cells, with P3HT as the hole transporting material, large  $V_{OC}$  values of up to 0.9 V were obtained, but overall efficiencies were low, around 0.002–0.031%. Germanium-based materials had higher  $V_{OC}$  values than the phosphine oxide-based molecules, and a larger proportion of fluoroarene groups improved device performance.

### Conclusion

Halogenation introduces polar bonds into  $\pi$ -conjugated materials. With electronegative fluorine and chlorine, the energy of the molecular orbitals is lowered with respect to their parent molecules, resulting in HOMO/LUMO levels that facilitate ambipolar or electron transport. In terms of bandgap engineering, the HOMO–LUMO gap can be decreased with chlorine, bromine and iodine functionalization; whereas in terms of crystal engineering, face-to-face

$\pi$ -stacking can dominate over the more pedestrian herringbone packing with partially fluorinated molecules.

Fluorination has been a route to electron transporting organic semiconductors for the past decade. Clearly, it lowers the charge injection barrier, introduces a certain barrier to ambient oxygen and water and stabilizes electron transport. With electron density inverted compared to their parent molecules, partially fluorinated conjugated molecules stack face to face, instead of edge to face, herringbone style.

Chlorinated molecules have been shown recently to work as well as fluorinated ones in terms of electron transport and device stability. This bodes well for the design and synthesis of novel organic semiconductors since such precursors are more readily available and chlorine chemistry is more developed. Aryl carbon–chlorine, bromine, and iodine bonds can be used to red shift the absorption. This has been attributed to both the inductive effect of halogens and the presence of empty d-orbitals on the halogen that allow the delocalization of the  $\pi$ -electron cloud. The trend with fluorine is less clear, as both red and blue shifts are observed with different molecules.

In summary, halogenation is a way to tune frontier energy levels and engineer molecular packing. It is a means to the larger goal of understanding the fundamental structure–property relationships that enable the rational design of organic semiconductors.

**Acknowledgment.** This work is supported by the Air Force Office of Scientific Research (FA9550-09-1-0256) and NSF Solid State Chemistry (DMR-0705687-002).

### References

- (1) Shirota, Y.; Kageyama, H. *Chem. Rev.* **2007**, *107*(4), 953–1010.
- (2) Walzer, K.; Maennig, B.; Pfeiffer, M.; Leo, K. *Chem. Rev.* **2007**, *107*(4), 1233–1271.

- (3) Murphy, A. R.; Frechet, J. M. J. *Chem. Rev.* **2007**, *107*(4), 1066–1096.
- (4) Zaumseil, J.; Sirringhaus, H. *Chem. Rev.* **2007**, *107*(4), 1296–1323.
- (5) Anthony, J. E. *Chem. Rev.* **2006**, *106*(12), 5028–5048.
- (6) Bao, Z.; Dodabalapur, A.; Lovinger, A. J. *Appl. Phys. Lett.* **1996**, *69*(26), 4108–4110.
- (7) Gunes, S.; Neugebauer, H.; Sariciftci, N. S. *Chem. Rev.* **2007**, *107*(4), 1324–1338.
- (8) Babudri, F.; Farinola, G. M.; Naso, F.; Ragni, R. *Chem. Commun.* **2007**, *10*, 1003–1022.
- (9) Wang, Y.; Herron, N.; Grushin, V. V.; LeCloux, D.; Petrov, V. *Appl. Phys. Lett.* **2001**, *79*(4), 449–451.
- (10) Pauling, L., *The Nature of the Chemical Bond*, 3rd ed.; Cornell University Press: Ithaca, NY, 1960.
- (11) Kerr, J. A. *Chem. Rev.* **1966**, *66*(5), 465–500.
- (12) Smyth, C. P., *Dielectric Behavior and Structure*; McGraw-Hill Book Company: New York, 1955.
- (13) Battaglia, M. R.; Buckingham, A. D.; Williams, J. H. *Chem. Phys. Lett.* **1981**, *78*, 421–423.
- (14) Steed, J. M.; Dixon, T. A.; Klemperer, W. J. *Chem. Phys.* **1979**, *70*(11), 4940–4946.
- (15) Williams, J. H. *Acc. Chem. Res.* **1993**, *26*(11), 593–598.
- (16) Ponzini, F.; Zagha, R.; Hardcastle, K.; Siegel, J. S. *Angew. Chem., Int. Ed.* **2000**, *39*(13), 2323–2325.
- (17) Cho, D. M.; Parkin, S. R.; Watson, M. D. *Org. Lett.* **2005**, *7*(6), 1067–1068.
- (18) Wang, Y. F.; Parkin, S. R.; Gierschner, J.; Watson, M. D. *Org. Lett.* **2008**, *10*(15), 3307–3310.
- (19) Sakamoto, Y.; Suzuki, T.; Kobayashi, M.; Gao, Y.; Fukai, Y.; Inoue, Y.; Sato, F.; Tokito, S. *J. Am. Chem. Soc.* **2004**, *126*(26), 8138–8140.
- (20) Sakamoto, Y.; Komatsu, S.; Suzuki, T. *J. Am. Chem. Soc.* **2001**, *123*(19), 4643–4644.
- (21) Ellman, B.; Nene, S.; Semyonov, A. N.; Twieg, R. J., *Adv. Mater.* **2006**, *18*(17), 2284–2288.
- (22) Delgado, M. C. R.; Pigg, K. R.; Filho, D.; Gruhn, N. E.; Sakamoto, Y.; Suzuki, T.; Osuna, R. M.; Casado, J.; Hernandez, V.; Navarrete, J. T. L.; Martinelli, N. G.; Cornil, J.; Sanchez-Carrera, R. S.; Coropceanu, V.; Bredas, J. L. *J. Am. Chem. Soc.* **2009**, *131*(4), 1502–1512.
- (23) Chen, H. Y.; Chao, I. *Chem. Phys. Lett.* **2005**, *401*(4–6), 539–545.
- (24) Salman, S.; Delgado, M. C. R.; Coropceanu, V.; Bredas, J. L. *Chem. Mater.* **2009**, *21*(15), 3593–3601.
- (25) Holmes, D.; Kumaraswamy, S.; Matzger, A. J.; Vollhardt, K. P. C. *Chem.—Eur. J.* **1999**, *5*(11), 3399–3412.
- (26) Mannsfeld, S. C. B.; Virkar, A.; Reese, C.; Toney, M. F.; Bao, Z. N. *Adv. Mater.* **2009**, *21*(22), 2294–2298.
- (27) Zhang, Y. X.; Cai, X.; Bian, Y. Z.; Li, X. Y.; Jiang, J. Z. *J. Phys. Chem. C* **2008**, *112*(13), 5148–5159.
- (28) Sanchez-Carrera, R. S.; Odom, S. A.; Kinnibrugh, T. L.; Sajoto, T.; Kim, E. G.; Timofeeva, T. V.; Barlow, S.; Coropceanu, V.; Marder, S. R.; Bredas, J. L. *J. Phys. Chem. B* **2010**, *114*(2), 749–755.
- (29) Sanchez-Carrera, R. S.; Coropceanu, V.; Kim, E. G.; Bredas, J. L. *Chem. Mater.* **2008**, *20*(18), 5832–5838.
- (30) Boese, R.; Miebach, T., **1996**.
- (31) Tang, M. L.; Oh, J. H.; Reichardt, A. D.; Bao, Z. N. *J. Am. Chem. Soc.* **2009**, *131*(10), 3733–3740.
- (32) Furuya, T.; Klein, J.; Ritter, T. *Synthesis* **2010**, *11*, 1804–1821.
- (33) Brown, J. M.; Gouverneur, V. *Angew. Chem., Int. Ed.* **2009**, *48*(46), 8610–8614.
- (34) Chen, Z. H.; Muller, P.; Swager, T. M. *Org. Lett.* **2006**, *8*(2), 273–276.
- (35) Swartz, C. R.; Parkin, S. R.; Bullock, J. E.; Anthony, J. E.; Mayer, A. C.; Malliaras, G. G. *Org. Lett.* **2005**, *7*(15), 3163–3166.
- (36) Tang, M. L.; Reichardt, A. D.; Miyaki, N.; Stoltenberg, R. M.; Bao, Z. N. *J. Am. Chem. Soc.* **2008**, *130*(19), 6064–6065.
- (37) Perepichka, D. F.; Bendikov, M.; Meng, H.; Wudl, F. *J. Am. Chem. Soc.* **2003**, *125*(34), 10190–10191.
- (38) Nyffeler, P. T.; Duron, S. G.; Burkart, M. D.; Vincent, S. P.; Wong, C. H. *Angew. Chem., Int. Ed.* **2005**, *44*(2), 192–212.
- (39) Subramanian, S.; Park, S. K.; Parkin, S. R.; Podzorov, V.; Jackson, T. N.; Anthony, J. E. *J. Am. Chem. Soc.* **2008**, *130*(9), 2706–2707.
- (40) Facchetti, A.; Yoon, M. H.; Stern, C. L.; Hutchison, G. R.; Ratner, M. A.; Marks, T. J. *J. Am. Chem. Soc.* **2004**, *126*(41), 13480–13501.
- (41) Ren, Y.; Dienes, Y.; Hettel, S.; Parvez, M.; Hoge, B.; Baumgartner, T. *Organometallics* **2009**, *28*(3), 734–740.
- (42) Heidenhain, S. B.; Sakamoto, Y.; Suzuki, T.; Miura, A.; Fujikawa, H.; Mori, T.; Tokito, S.; Taga, Y. *J. Am. Chem. Soc.* **2000**, *122*(41), 10240–10241.
- (43) Facchetti, A.; Yoon, M. H.; Stern, C. L.; Katz, H. E.; Marks, T. J. *Angew. Chem., Int. Ed.* **2003**, *42*(33), 3900–3903.
- (44) Okamoto, K.; Ogino, K.; Ikari, M.; Kunugi, Y. *Bull. Chem. Soc. Jpn.* **2008**, *81*(4), 530–535.
- (45) Wang, Y. F.; Watson, M. D. *J. Am. Chem. Soc.* **2006**, *128*(8), 2536–2537.
- (46) Schmidt, R.; Oh, J. H.; Sun, Y. S.; Deppisch, M.; Krause, A. M.; Radacki, K.; Braunschweig, H.; Konemann, M.; Erk, P.; Bao, Z. A.; Wurthner, F. *J. Am. Chem. Soc.* **2009**, *131*(17), 6215–6228.
- (47) Gsanger, M.; Oh, J. H.; Konemann, M.; Hoffken, H. W.; Krause, A. M.; Bao, Z. N.; Wurthner, F. *Angew. Chem., Int. Ed.* **2009**, *49*(4), 740–743.
- (48) Suraru, S. L.; Wurthner, F. *Synthesis* **2009**, *11*, 1841–1845.
- (49) Yuan, Z. Y.; Li, J.; Xiao, Y.; Li, Z.; Qian, X. H. *J. Org. Chem.* **2010**, *75*(9), 3007–3016.
- (50) Garnier, F.; Yassar, A.; Hajlaoui, R.; Horowitz, G.; Deloffre, F.; Servet, B.; Ries, S.; Alnot, P. *J. Am. Chem. Soc.* **1993**, *115*(19), 8716–8721.
- (51) Facchetti, A.; Mushrush, M.; Yoon, M. H.; Hutchison, G. R.; Ratner, M. A.; Marks, T. J. *J. Am. Chem. Soc.* **2004**, *126*(42), 13859–13874.
- (52) Yoon, M. H.; DiBenedetto, S. A.; Facchetti, A.; Marks, T. J. *J. Am. Chem. Soc.* **2005**, *127*(5), 1348–1349.
- (53) Le, Y.; Umemoto, Y.; Okabe, M.; Kusunoki, T.; Nakayama, K. I.; Pu, Y. J.; Kido, J.; Tada, H.; Aso, Y. *Org. Lett.* **2008**, *10*(5), 833–836.
- (54) Vidolot-Ackermann, C.; Brisset, H.; Zhang, J.; Ackermann, J.; Nenon, S.; Fages, F.; Marsal, P.; Tanisawa, T.; Yoshimoto, N. *J. Phys. Chem. C* **2009**, *113*(4), 1567–1574.
- (55) Yoon, M. H.; Facchetti, A.; Stern, C. E.; Marks, T. J. *J. Am. Chem. Soc.* **2006**, *128*(17), 5792–5801.
- (56) Koh, S. E.; Risko, C.; da Silva, D. A.; Kwon, O.; Facchetti, A.; Bredas, J. L.; Marks, T. J.; Ratner, M. A. *Adv. Funct. Mater.* **2008**, *18*(2), 332–340.
- (57) Ie, Y.; Nitani, M.; Uemura, T.; Tominari, Y.; Takeya, J.; Honsho, Y.; Saeki, A.; Seki, S.; Aso, Y. *J. Phys. Chem. C* **2009**, *113*(39), 17189–17193.
- (58) Crouch, D. J.; Skabara, P. J.; Lohr, J. E.; McDouall, J. J. W.; Heeney, M.; McCulloch, I.; Sparrowe, D.; Shkunov, M.; Coles, S. J.; Horton, P. N.; Hursthouse, M. B. *Chem. Mater.* **2005**, *17*(26), 6567–6578.
- (59) Ando, S.; Murakami, R.; Nishida, J.; Tada, H.; Inoue, Y.; Tokito, S.; Yamashita, Y. *J. Am. Chem. Soc.* **2005**, *127*(43), 14996–14997.
- (60) Ando, S.; Nishida, J. I.; Tada, H.; Inoue, Y.; Tokito, S.; Yamashita, Y. *J. Am. Chem. Soc.* **2005**, *127*(15), 5336–5337.
- (61) Entani, S.; Kaji, T.; Ikeda, S.; Mori, T.; Kikuzawa, Y.; Takeuchi, H.; Saiki, K. *J. Phys. Chem. C* **2009**, *113*(15), 6202–6207.
- (62) Yagodkin, E.; Xia, Y.; Kalihari, V.; Frisbie, C. D.; Douglas, C. J. *J. Phys. Chem. C* **2009**, *113*(37), 16544–16548.
- (63) Moon, H.; Zeis, R.; Borkent, E. J.; Besnard, C.; Lovinger, A. J.; Siegrist, T.; Kloc, C.; Bao, Z. N. *J. Am. Chem. Soc.* **2004**, *126*(47), 15322–15323.
- (64) Okamoto, T.; Senatore, M. L.; Ling, M. M.; Mallik, A. B.; Tang, M. L.; Bao, Z. N. *Adv. Mater.* **2007**, *19*(20), 3381–3384.
- (65) Tang, M. L.; Reichardt, A. D.; Wei, P.; Bao, Z. N. *J. Am. Chem. Soc.* **2009**, *131*(14), 5264–5273.
- (66) Tang, M. L.; Reichardt, A. D.; Okamoto, T.; Miyaki, N.; Bao, Z. A. *Adv. Funct. Mater.* **2008**, *18*(10), 1579–1585.
- (67) Tang, M. L.; Reichardt, A. D.; Siegrist, T.; Mannsfeld, S. C. B.; Bao, Z. N. *Chem. Mater.* **2008**, *20*(14), 4669–4676.
- (68) Ling, M. M.; Bao, Z. N.; Erk, P. *Appl. Phys. Lett.* **2006**, *89*, 16.
- (69) Bao, Z. A.; Lovinger, A. J.; Brown, J. *J. Am. Chem. Soc.* **1998**, *120*(1), 207–208.
- (70) Ling, M. M.; Erk, P.; Gomez, M.; Koenemann, M.; Locklin, J.; Bao, Z. N. *Adv. Mater.* **2007**, *19*(8), 1123–1127.
- (71) Schmidt, R.; Ling, M. M.; Oh, J. H.; Winkler, M.; Konemann, M.; Bao, Z. N.; Wurthner, F. *Adv. Mater.* **2007**, *19*, 3692–3695.
- (72) Katz, H. E.; Johnson, J.; Lovinger, A. J.; Li, W. J. *J. Am. Chem. Soc.* **2000**, *122*(32), 7787–7792.
- (73) Jones, B. A.; Facchetti, A.; Wasielewski, M. R.; Marks, T. J. *J. Am. Chem. Soc.* **2007**, *129*(49), 15259–15278.
- (74) Katz, H. E.; Lovinger, A. J.; Johnson, J.; Kloc, C.; Siegrist, T.; Li, W.; Lin, Y. Y.; Dodabalapur, A. *Nature* **2000**, *404*(6777), 478–481.
- (75) Weitz, R. T.; Amsharov, K.; Zschieschang, U.; Villas, E. B.; Goswami, D. K.; Burghard, M.; Dosch, H.; Jansen, M.; Kern, K.; Klauk, H. *J. Am. Chem. Soc.* **2008**, *130*(14), 4637–4645.
- (76) Oh, J. H.; Sun, Y. S.; Schmidt, R.; Toney, M. F.; Nordlund, D.; Konemann, M.; Wurthner, F.; Bao, Z. A. *Chem. Mater.* **2009**, *21*(22), 5508–5518.
- (77) Chikamatsu, M.; Itakura, A.; Yoshida, Y.; Azumi, R.; Yase, K. *Chem. Mater.* **2008**, *20*(24), 7365–7367.
- (78) Wobkenberg, P. H.; Ball, J.; Bradley, D. D. C.; Anthopoulos, T. D.; Kooistra, F.; Hummelen, J. C.; de Leeuw, D. M. *Appl. Phys. Lett.* **2008**, *92*, 14.
- (79) Geramita, K.; Tao, Y. F.; Segalman, R. A.; Tilley, T. D. *J. Org. Chem.* **2010**, *75*(6), 1871–1887.
- (80) Geramita, K.; McBee, J.; Tao, Y. F.; Segalman, R. A.; Tilley, T. D. *Chem. Commun.* **2008**, *41*, 5107–5109.